Characterization of the E(0.31) defect introduced in bulk *n*-Ge by H or He plasma exposure

C. Nyamhere,[1,a)] A. Venter,[1] F. D. Auret,[2] S. M. M. Coelho,[2] and D. M. Murape[1]
[1]*Department of Physics, Nelson Mandela Metropolitan University, P.O. Box 77000, Port Elizabeth 6031, South Africa*
[2]*Department of Physics, University of the Pretoria, Lynnwood Road, Pretoria 0002, South Africa*

(Received 29 September 2011; accepted 21 January 2012; published online 29 February 2012)

Bulk antimony (Sb) doped germanium (*n*-Ge) samples with doping concentrations ranging between $7.0 \times 10^{14}\,cm^{-3}$ and $2.5 \times 10^{15}\,cm^{-3}$ were exposed to a dc-hydrogen or helium plasma. Hydrogen exposure resulted in the introduction of a single prominent defect level at $E_C - 0.31\,eV$. Exposing similar samples to He plasmas introduced the same electron trap. The trap concentration increased linearly with dopant concentration suggesting that Sb may be a component of this plasma-induced trap. Thermal annealing kinetics studies suggested that this defect anneals out by diffusion. © *2012 American Institute of Physics*. [doi:10.1063/1.3687426]

I. INTRODUCTION

The profound interaction of hydrogen with defects and dopants in semiconductors is well documented and since device development and performance is intimately related to defect engineering, the study of the interaction of hydrogen with defects is of vital technological importance. Hydrogen (H) can be introduced into semiconductors either unintentionally during growth and/or chemical processing or intentionally by hydrogen plasmas.[1,2] Although much is known about the behavior of H in Si and GaAs,[3,4] the picture as far as germanium (Ge) is concerned, is not as complete. Ge of late has been receiving renewed attention for, in particular, its superior low-field electron and hole mobility and also higher dielectric constant when compared to silicon,[5] rendering it a possible high-κ candidate material (to replace dielectric silicon dioxide gates) for further miniaturization of microelectronic components.[6] The relatively small bandgap of Ge also makes it potentially useful for gamma-ray detection. "Pure" Ge epitaxial layers are however required for this purpose. It has been shown that undesired deep level recombination can be curtailed through the passivation of deep impurities by H-plasma treatment. While hydrogen plasma treatment is known to de-activate shallow and/or deep levels, it is also known to introduce new traps. A recent review on the role of hydrogen in Ge was presented by Weber *et al.*[2]

Several authors have studied the effect of hydrogen in Ge by exposing the material to H-plasmas. Experimental proof of passivation of shallow donors has been reported by (among others) Bollmann *et al.*[7] While the passivation of, in particular, transition metal related deep levels in Ge at passivation temperatures exceeding 200 °C has been reported extensively,[8–10] to the best of our knowledge helium (He) plasma induced defects have not yet been reported. This paper reports on defects introduced in *n*-Ge, of varying doping concentration, following dc-H or dc-He plasma treatment.

II. EXPERIMENTAL PROCEDURE

Bulk grown *n*-type Ge samples supplied by Umicore, doped with antimony (Sb) to a free carrier density of $7.0 \times 10^{14}\,cm^{-3}$, $1.0 \times 10^{15}\,cm^{-3}$, and $2.5 \times 10^{15}\,cm^{-3}$, labeled as sample A, B, and C, respectively, have been used in this study. Prior to metallization, samples (1 cm × 0.5 cm) were degreased successively in trichloroethylene, acetone, and methanol. Following this, the samples were etched in a mixture of H_2O_2:H_2O (1:5) for 1 min before rinsing in deionized (DI) water and blown-dry in flowing N_2. Ohmic contacts were next fabricated by resistively evaporating a 130 nm AuSb (0.6% Sb) layer onto the backside of the sample followed by annealing at 350 °C for 10 min in a 99.999% argon (Ar) atmosphere. The samples were again chemically cleaned as described above and then immediately exposed to a dc hydrogen or helium plasma (described in detail in Ref. 11). During plasma exposure, the sample temperature was held at 100 °C while the chamber vacuum was maintained at 0.2 mbar or 0.4 mbar for He or H plasma, respectively. A summary of the samples and the respective plasma processes are listed in Table I.

Next Schottky barrier diodes (SBDs) were fabricated on the front surface of the passivated samples (for samples A, B, C, and C′). This was preceded by a 2 min etch in HF:HNO_3 (1:1) to remove the heavily damaged near surface region for better contact quality. The etching rate was 58 nm/min, and a layer of 116 nm (0.12 μm) was removed after etching for 2 min. Immediately after this, Pd SBDs, 0.5 mm in diameter and 100 nm thick, were resistively deposited through a metal shadow mask. For experimental control purposes a sample was also exposed to molecular H or He in the plasma system (without forming a plasma) at 100 °C before SBD fabrication. In addition to this, a hydrogenated sample was further irradiated (after SBD fabrication) with MeV electrons with a fluence of $5.9 \times 10^{13}\,e/cm^2$ at room temperature (sample C″).

[a)]Author to whom correspondence should be addressed. Electronic mail: cloud.nyamhere@nmmu.ac.za. Present address: Physics Department, Nelson Mandela Metropolitan University, P.O. Box 77000, Port Elizabeth 6031, South Africa. Fax: +27 41 504 1989.

TABLE I. Sample details and plasma processes.

Sample	N_d (cm^{-3})	Plasma used	Exposure time
Sample A	7.0×10^{14}	dc-hydrogen	10 min.
Sample B	1.0×10^{15}	dc-hydrogen	10 min.
Sample C	2.5×10^{15}	dc-hydrogen	10 min.
Sample C′ (used sample C)	2.5×10^{15}	dc-helium	10 min.
Sample C″ (used sample C)	2.5×10^{15}	dc-hydrogen + MeV electron irradiation	
Reference (used samples A, B, or C)		No plasma or no MeV electrons exposure	

Room temperature (RT) current-voltage (*I-V*) and capacitance-voltage (*C-V*) measurements were used to assess the SBD quality and monitor the free carrier concentration of the respective plasma exposed samples. Deep levels introduced by the respective plasmas and subsequent MeV electron irradiation were characterized by deep level transient spectroscopy (DLTS) and Laplace-DLTS.[12,13] The *signatures* of the observed deep levels (i.e., activation energy for electron emission, E_T, and the apparent capture cross section, σ_a), were determined from Arrhenius plots of $ln(T^2/e)$ versus 1000/T. Here, *e* represents the electron emission rate, and *T* the measurement temperature in Kelvin. In addition, the thermal behavior of the defect introduced by the H or He-plasma was studied by annealing the samples isochronally (10 min) between RT and 300 °C in an Ar ambient.

III. RESULTS AND DISCUSSION

A. Defects introduced in *n*-Ge after hydrogen or helium plasma exposure

Figure 1 depicts DLTS spectra of (a) the reference sample, and after exposure to (b) a dc-H plasma, (c) a dc-He plasma, (d) an inductively coupled Ar plasma (ICP) (reproduced from Ref. 14) and (e) a dc-H plasma + MeV electron irradiation. Evidently the reference sample did not contain any deep defect levels within the detection limit of the DLTS system. Following dc-H plasma treatment, (Fig. 1(b)), a single electron trap E(0.31) with peak position around 156 K is observed. The same defect is apparently observed after He plasma treatment, and Auret *et al.*[14] also observed a similar defect after Ar ICP etching of similar samples, Figs. 1(c) and 1(d), respectively. All the electronic properties of these traps (obtained from the Arrhenius plots depicted in Fig. 2 and annealing studies) are summarized in Table II. It should be noted that, no hole traps were observed under forward bias injection pulse conditions after plasma exposure. The H-plasma related defect has an activation energy of 0.31 ± 0.01 eV below the conduction band with an apparent capture cross section of about 2.0×10^{-14} cm^2. As is clear from Fig. 2, the same signatures are observed for this defect after He and Ar plasmas. These results suggest that although hydrogen is involved in the formation of the E(0.31), it is not necessarily a constituent of this complex as suspected in our earlier report.[15] It should also be noted that Lauwaert *et al.*[9] observed a single electron trap level at $E_C - 0.237$ eV in *n*-Ge doped to 8×10^{14} cm^{-3} (dopant not specified), after passivation with H-plasma at a vacuum pressure of 6.10 Pa (0.061 mbar), sample temperature of 150 °C and exposure time of 2.5 hr. The difference in trap activation energy suggests that a different complex is formed as a result of possibly different dopants.

It is interesting, but not surprising, to note that after irradiating the hydrogenated samples with MeV electrons from a strontium (Sr^{90}) nuclide source,[16] the electron trap E(0.38), a double acceptor charge state (–/-) of the V-Sb defect (E-center), is introduced as shown in Fig. 1(e). This is expected for Ge (Refs. 17 and 18) after high energy particle irradiation. This is clear evidence that MeV irradiation causes the formation of single vacancies and interstitials, resulting in the formation of the E(0.38) complex. The spectrum of the single acceptor charge state of the E-center, i.e., (-/0), with activation energy $E_V + 0.30$ eV, usually observed peaking at a temperature of around 142 K, is distorted by the strong presence of $E_C + 0.31$ eV (E(0.31)) defect as shown by the DLTS spectra in Fig. 3. No other irradiation induced defects in significant concentrations were observed after MeV electron irradiation.

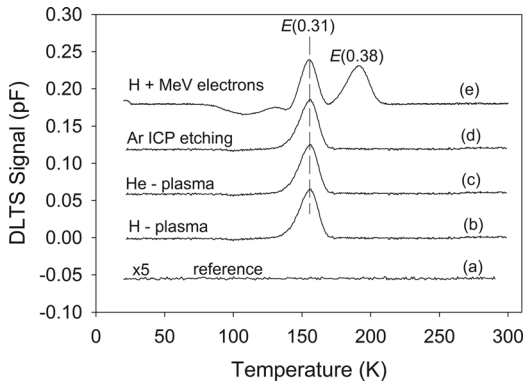

FIG. 1. DLTS spectra of (a) the reference sample and after exposure to (b) a dc-hydrogen plasma, (c) a dc-He plasma, (d) Ar ICP etching, and (e) a dc-hydrogen plasma + MeV electrons. The spectra were recorded using a reverse bias (V_r) of −2 V, filling pulse voltage (V_p) of 0 V superimposed on the reverse bias while the rate window was 80 s^{-1}.

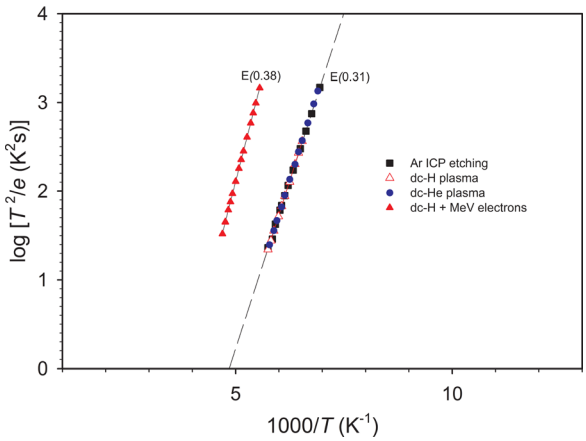

FIG. 2. (Color online) Arrhenius plots for the E(0.31) trap after exposing *n*-Ge to the H plasma (open triangles), He plasma (filled circles) or Ar ICP plasmas (filled squares) re-plotted from Ref. 14 and the E(0.38) trap introduced after dc-H plasma + MeV electron irradiation (filled triangles).

TABLE II. Summary of electronic properties of defects in *n*-Ge after H, He, Ar plasma and H-plasma + MeV electrons irradiation.

Defect	E_T (±0.01) (eV)	σ_a (±10%) (cm^{-2})	T^a_{peak} (K)	T^b_{out} (°C)	Defect identity
		H-plasma			
E (0.31)	$E_C - 0.31$	2.0×10^{-14}	156	250	Sb-related
		He-plasma			
E(0.31)	$E_C - 0.31$	2.0×10^{-14}	156	250	Sb-related
		Ar-ICP etching			
$EP_{0.31}$	$E_C - 0.31$	1.3×10^{-14}	156	250	Reference 14
		H-plasma + MeV electrons			
E(0.38)	$E_C - 0.38$	6.6×10^{-14}	191	200	V-Sb$^{-/-}$ (Refs. 17 and 18)

[a]Peak temperature at a rate window of 80 s^{-1}.
[b]Temperature at which defect is completely annealed-out.

B. E(0.31) concentration dependence on Sb doping levels

Figure 4 depicts *C-V* depth profiles of the (a) reference (b) He-plasma exposed (25 min), and H-plasma exposed (25 min) samples. These profiles clearly show that the free carrier density, after exposure to the H-plasma for 25 min, is reduced by ~1.5 orders of magnitude, which can be explained by passivation of shallow donors. This explanation is supported by the fact that annealing (as discussed in detail in our earlier report[15]) partially recovers the free carrier concentration of the passivated sample. This is contrary to what is observed after He plasma exposure for which the introduction of E(0.31) is responsible for the small decrease in the free carrier concentration.

In order to gain more insight into the origin of the E(0.31) defect, Ge samples of different doping concentrations (samples A, B, and C) have been exposed to H plasmas employing the plasma conditions described in Table I. The resulting defect concentration depth profiles for the samples with different doping levels are depicted in Fig. 5.

The trap concentration profiles were calculated, using the fixed bias-variable pulse method with transition region (lambda) correction.[19] The trap depth profiles show a progressive decrease with depth within the region probed, suggesting that this trap is a consequence of the bombardment of the near-surface region with the plasma species. It should also be noted that although a reverse bias of −5 V has been used for all the depth profile measurements, different depth regions have been probed due to the dependence of the depletion width, *w*, on the doping concentration as given by

$$W = \sqrt{\frac{2\varepsilon_s}{qN_d}(V_{bi} - V_a)}, \quad (1)$$

where ε_s is semiconductor permittivity, V_{bi}, the built in potential, V_a, the applied bias, q, the electron charge, and N_d, the uncompensated doping concentration. Figure 6 depicts the defect concentration as a function of doping concentration. The linear dependence of the defect concentration with the Sb doping levels is clearly evident, suggesting that this defect is related to Sb. The absence of vacancy (V) or interstitial (I)-related defects normally observed in similar samples after high energy electron or proton irradiation shows that V-I pairs, as well as single vacancies and interstitials, are not created by plasma exposure in these samples. This leaves C, O, or higher order vacancy complexes V_n, where, $n > 2$, in the semiconductor as the possible candidates for this defect formation.

C. Annealing kinetics of E(0.31)

The thermal annealing kinetics of E(0.31), is presented next. Generally defect annealing mechanisms can be classified into two main categories.

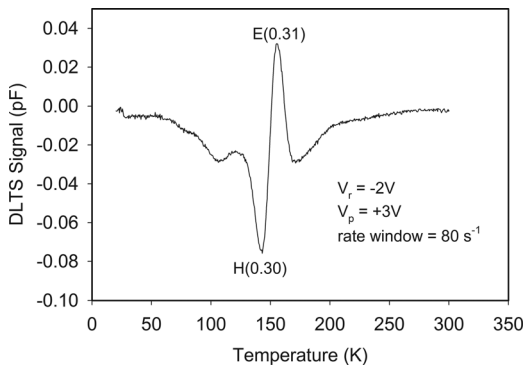

FIG. 3. DLTS spectra of the Ge sample after dc-hydrogen plasma + MeV electrons exposure, showing distortion for both E(0.31) and hole trap. The spectra were recorded using a reverse bias (V_r) of −2 V, filling pulse voltage (V_p) of + 3 V superimposed on the reverse bias while the rate window was 80 s^{-1}.

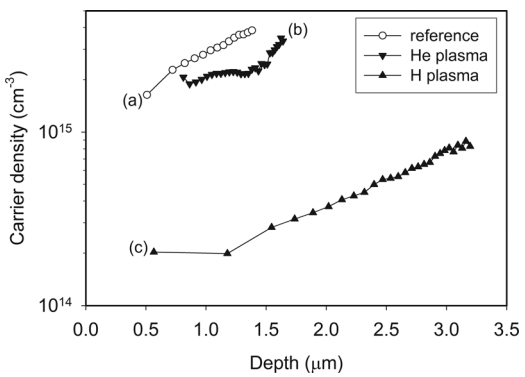

FIG. 4. *C-V* depth profiles of (a) the reference (no plasma exposure) and after exposure to (b) He-plasma (sample Ć) and (c) H-plasma (sample C) *n*-Ge samples. In each case, the plasma exposure time was 25 min.

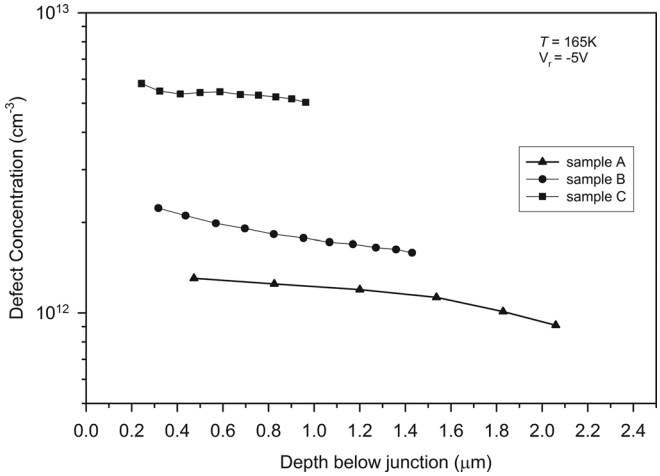

FIG. 5. The concentration depth profiles of E(0.31) for sample A, B, and C, respectively, after hydrogen plasma exposure at similar plasma conditions for a period of 10 min at 100 °C. The spectra were recorded at a quiescent reverse bias of −5 V, a varying pulse height (fixed bias-variable pulse method (Ref. 19)) and pulse width of 1 ms.

(i) Diffusion, i.e., as the sample temperature is increased defects migrate/diffuse to a sink (such as the surface or grain boundaries) or they are subsequently trapped by other defects or impurities to form completely new defects.
(ii) Dissociation, i.e., which is simply a separation of the constituents forming the defect complex.

These annealing mechanisms have a characteristic activation energy (E_a). At a fixed annealing temperature (T_a) the annealing kinetics can be deduced by monitoring the decrease in defect concentration as a function of time and can provide information on the defect distribution and the associated annealing mechanism. As such it provides valuable supplementary information on the identity and/or origin of defects. Typically, in a sample with defect concentration N_T, the number of defects that anneal per unit time is proportional to the number of defect $N_T(t)$ present at time t. The annealing rate can consequently be expressed as

$$\frac{dN_T}{dt} = Kf(N_T), \tag{2}$$

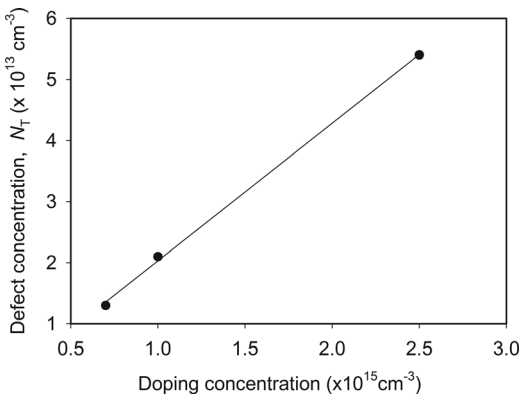

FIG. 6. Defect concentration of E(0.31) vs doping concentration for *n*-Ge after hydrogen passivation. The defect concentrations were recorded at a depth of 0.5 μm below the semiconductor surface.

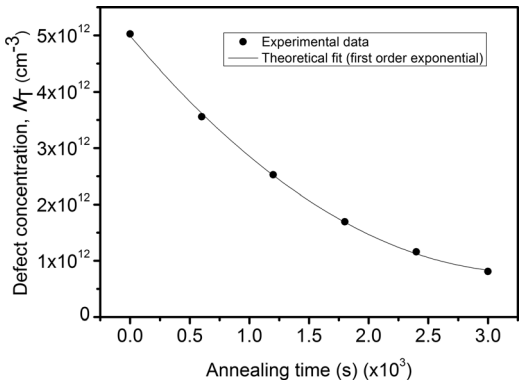

FIG. 7. Defect concentration of E(0.31) vs annealing time recorded at 160 °C. The solid line represents the first order exponential fit.

where K is the annealing rate constant. If the function $f(N_T) = N_T$ then the annealing kinetics is said to be of first order and second order if $f(N_T) = N_T^2$. Assuming first order kinetics, solving Eq. (2) yields

$$N_T(t) = N_T(0)exp(-Kt), \tag{3}$$

where $N_T(0)$ is the initial defect concentration at $t = 0$. The annealing rate constant given in Eqs. (2) and (3) has the form

$$K(T) = K_0 exp(E_a/k_B T), \tag{4}$$

where k_B is the Boltzmann constant, K_0 is a pre-exponential constant (which contains the vibrational frequency associated with the annealing process) and E_a is the activation energy of the annealing process. In order to determine the annealing activation energy, the variation of N_T versus annealing time (t) is measured at constant temperature, say T_1 and a plot of $ln(N_T)$ versus t will yield a straight line (for first order kinetics) from which the rate constant K_1 is extracted. If these measurements are repeated for constant temperatures T_2, T_3, T_4 etc, then rate constants K_2, K_3, K_4 etc are extracted, respectively. From Eq. (3) an Arrhenius plot of ln(K) versus 1/T will yield the annealing activation energy E_a (from the gradient) and pre-exponential constant K_0 (from the vertical axis intercept).

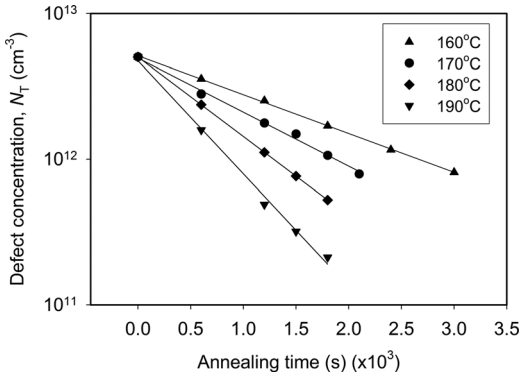

FIG. 8. Defect concentration vs annealing time measured at temperatures 160 °C, 170 °C, 180 °C, and 190 °C from which the annealing rate constant K is extracted. The solid lines represent the least squares fits of the experimental data.

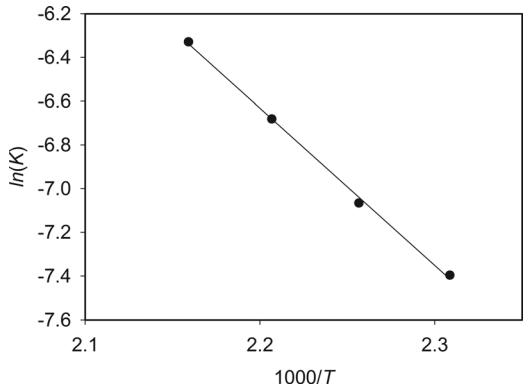

FIG. 9. The Arrhenius plot of the *ln*(K) vs 1000/T from which the annealing activation energy and pre-exponential factors are extracted.

The annealing of E(0.31) at temperatures above 160 °C follows a first order decay process as evidenced by the experimental data and first order exponential theoretical fit in Fig. 7. The defect concentrations as a function of annealing time for annealing temperatures (160 °C, 170 °C, 180 °C, and 190 °C) are depicted in Fig. 8, from which the annealing rate for each temperature was extracted. Figure 9 depicts the temperature dependent rate constant from which the activation energy ($E_a = 0.62$ eV) and a pre-exponential factor $K_0 = 1.8 \pm 1.0 \times 10^4\,s^{-1}$ were extracted. The small value of pre-exponential factor, $<10^{12}\,s^{-1}$ points to a diffusion driven annealing mechanism,[20,21] although it is not yet clear whether the E(0.31) trap will eventually dissociate at higher temperatures or it simply diffuses out of the sample.

IV. SUMMARY

The hydrogen, helium, or Ar plasmas exposure of *n*-Ge resulted in the formation of the same electron trap (E(0.31)). This confirms that hydrogen, although involved in its formation, is not a constituent of this defect. In addition, the E(0.31) concentration as a function of Sb doping concentration shows a linear dependence suggesting that Sb is a constituent of this defect complex. After irradiating the hydrogen passivated sample with MeV electrons, the E-center is introduced. The annealing kinetics of E(0.31) trap suggests that it anneals by diffusion. Further work, especially on determining its physical model, is required to unambiguously identify this plasma induced trap.

ACKNOWLEDGMENTS

This work was based upon research supported by the South African Research Chair's Initiative of the Department of Science and Technology, National Research Foundation, as well as by the Nelson Mandela Metropolitan University (NMMU).

[1]R. Jones, Philos. Trans. R. Soc. London A. **350**, 189 (1995).
[2]J. Weber, M. Miller, and E. V. Lavrov, Mater. Sci. Semicond. Process **9**, 564 (2006).
[3]S. J. Pearton, J. W. Corbett, and M. Stavola, Adv. Mater. **4**, 332 (1992).
[4]P. C. Srivastava and U. P. Singh, Bull. Mater. Sci. **19**, 51 (1996).
[5]*Germanium Silicon, Physics and Materials, Semiconductor and Semi-metals*, Vol. **56**, edited by Hull and J. C. Bean (Academic, San Diego, 1999).
[6]P. C. McIntyre, D. Chi, C. O. Chui, H. Kim, K. I. Seo, K. C. Saraswat, R. Sreenivasan, T. Sugawara, F. S. Aguirre-Testado, and R. M. Wallace, ECS Trans. **3**, 519 (2006).
[7]J. Bollmann, R. Endler, V. T. Dung, and J. Weber, Physica B **404**, 5099 (2009).
[8]S. J. Pearton, A. J. Tavendale, J. M. Kahn, E. E. Haller, Rad. Effects Defects Solids **81**, 293 (1984).
[9]J. Lauwaert, M. F. Beaufort, E. Simoen, D. Depla, and P. Clauws, Mater. Sci. Semicond. Process **9**, 571 (2006).
[10]J. Lauwaert, J. Van Gheluwe, and P. Clauws, Mater. Sci. Semicond. Process **11**, 360 (2008).
[11]C. Nyamhere, J. R. Botha, and A. Venter, Physica B **406**, 2273 (2011).
[12]L. Dobaczewski, P. Kaczor, I. D. Hawkins, and A. R Peaker, J. Appl. Phys. **76**, 194 (1994).
[13]L. Dobaczewski, A. R Peaker, and K. B. Nielsen, J. Appl. Phys. **96**, 4689 (2004).
[14]F. D. Auret, S. M. M. Coelho, G. Myburg, P. J. van Rensburg, and W. E. Meyer, Thin Solid Films **518**, 2485 (2010).
[15]C. Nyamhere, A. Venter, D. M. Murape, F. D. Auret, S. M. M. Coelho, and J. R. Botha, "dc-Hydrogen plasma induced defects in bulk n-Ge," Physica B (to be published).
[16]F. D. Auret, S. A. Goodman, G. Myburg, and W. E. Meyer, Appl. Phys. A **56**, 547 (1993).
[17]V. P. Makervich, A. R. Peaker, V. V. Litvinov, V. V. Emstev, and L. I. Murin, J. Appl. Phys. **95**, 4078 (2004).
[18]F. D. Auret, W. E. Meyer, S. Coelho, and M. Hayes, Appl. Phys. Lett. **88**, 242110 (2006).
[19]Y. Zohta and M. O. Watanabe, J. Appl. Phys. **53**, 1809 (1982).
[20]M. Mikelsen, E. V. Monakhov, G. Alfieri, B. S. Avset, and B. G. Svensson, Phys. Rev. B **72**, 195207 (2005).
[21]F. D. Auret and P. N. K. Deenapanray, Crit. Rev. Solid State Mater. Sci. **29**, 1 (2004).